Title

Estimating the impact of tariff-driven behind-the-meter storage operation on distribution grid investments

Journal

Energy Reports, 16

ISSN

2352-4847

Authors

Rodriguez-Garcia, Luis
Barbose, Galen
Forrester, Sydney
et al.

Publication Date

2026-12-01

DOI

10.1016/j.egyr.2026.109531

Energy Reports 16 (2026) 109531

Contents lists available at ScienceDirect

Energy Reports

journal homepage: www.elsevier.com/locate/egyr

Research paper

Estimating the impact of tariff-driven behind-the-meter storage operation on distribution grid investments

Luis Rodriguez-Garcia [a],*, Galen Barbose [a], Sydney Forrester [a], Michael Blonsky [b], Miguel Heleno [a]

[a] Lawrence Berkeley National Laboratory, Berkeley, CA, USA
[b] EnergyHub, Brooklyn, NY, USA

ARTICLE INFO

Keywords:
Distribution grid
Grid expansion
Distributed energy resources
Tariff structure
Battery energy storage

ABSTRACT

Increasing growth of distributed solar photovoltaics (PV) and electric vehicles (EV) can strain local distribution networks and require costly upgrades. Distributed battery storage, often deployed alongside PV, can be used to mitigate those costs, depending on how batteries are operated. This study evaluates the potential deferral value of distributed battery storage across a range of tariff structures, focusing on the rate structures most commonly available to residential customers today and related variants. Deferrals are evaluated with a least-cost distribution grid expansion optimization model to identify requirements on line reconductoring, transformer upgrades, and voltage regulator installations under each tariff. Results show that TOU rates and net billing tariffs can yield meaningful deferral value, depending on specific tariff structure features. Under the best performing tariff structure tested, storage produced a median annualized deferral value of \$7.18 per kW of storage capacity (kW_S) across all feeders in the sample, though deferral values were considerably larger for feeders with peak loads that coincide with utility system peak, i.e., timing of TOU peak period. In contrast, under an unrestricted TOU design with no restrictions on grid charging or discharging, the median deferral value was \$0/kW_S illustrating the critical importance of tariff structure details.

1. Introduction

Electric utility expenditures on distribution system investments have been the leading source of rising electricity rates in recent years, straining consumer pocketbooks and challenging energy affordability (Forrester et al., 2024). Though the underlying drivers for those investments are numerous, distributed solar photovoltaics (PV) (Palmintier et al., 2016), electric vehicles (EVs) (McAllister et al., 2019), and other forms of distributed generation (Ackermann and Knyazkin, 2002) are significant contributors to increasing distribution grid stress. The rapid growth of these technologies raises concerns about PV spatial distribution and integration costs (K.A. Horowitz et al., 2018), as well as their impact on hosting capacity and costs, depending on the size of adopted PV (K.A.W. Horowitz et al., 2018). Several studies have pointed out the effects of electrification on load forecasting (California Public Utilities Commission, 2023), infrastructure spending (U.S. Energy Information Administration, 2024), where distribution investment becomes the largest expenditure across sectors (Edison Electric Institute, 2024). In parallel with PV adoption, distributed battery storage has also begun to proliferate as an enabling technology for integrating PV (Hill et al., 2012) and other variable renewable source integration (Koivisto et al., 2019), mitigating voltage-related issues (Babacan et al., 2017), supporting the electrification of transportation and heating through EVs and heat pumps (Gupta et al., 2021), and expanding distribution grid hosting capacity (Lee et al., 2020). Accordingly, recent studies have explored approaches to the optimal siting of storage systems (Okafor et al., 2025), their sizing (Su et al., 2025), and potentially maximizing their benefits through revenue optimization (Dennis et al., 2025).

Currently in the U.S., residential battery storage systems are operated primarily under one of two basic tariff structures: time-of-use (TOU) rates or net billing tariffs. Under TOU rates, customers use their battery storage to arbitrage between peak and off-peak pricing periods. On the other hand, under net billing, customers use battery storage to shift surplus solar production from the middle of the day to evening and night-time hours, arbitraging between the grid export rate and the higher retail price for consumption. In the case of TOU rates, customers with storage are incentivized to discharge during peak TOU hours, which can help to reduce overloading and alleviate undervoltages caused by added EV demand and other sources of load

* Corresponding author.
E-mail address: luisrodriguezgarcia@lbl.gov (L. Rodriguez-Garcia).

https://doi.org/10.1016/j.egyr.2026.109531
Received 20 January 2026; Received in revised form 30 May 2026; Accepted 5 July 2026
Available online 20 July 2026

growth during those hours (Alam et al., 2013). In the case of net billing rates, customers with storage are incentivized to charge during hours when their PV system would otherwise export to the grid, mitigating overvoltages caused by high PV grid injections across the feeder (Koivisto et al., 2019).

That being said, those benefits may be offset because the pricing signals under these tariffs are fairly coarse and may be misaligned with the times of greatest need on any individual feeder. In the case of TOU rates, peak pricing periods are based on the overall utility system peak, which may not coincide with peak loads on any individual feeder, encouraging discharge at ineffective times. Net billing faces an analogous mismatch when the availability of surplus solar for storage charging by individual customers does not align well with the times of most severe overvoltage on the feeder (Morell-Dameto et al., 2024). While TOU rates and net billing structures are generally considered practical volumetric price signals with known benefits in encouraging battery storage operations and demand response, the reduction in distribution system upgrade needs in the presence of high PV and battery penetration depends on how battery operation aligns with feeder constraints (Morell Dameto et al., 2020). Therefore, understanding the potential for TOU rates and net billing to address the distribution impacts of high PV and EV penetrations is far from straightforward.

To address that knowledge gap, this paper compares the distribution system investment cost savings from residential battery storage under a range of TOU-based tariff structures and net billing, in conjunction with relatively high levels of distributed solar and EVs. The analysis relies on a least-cost optimization for distribution grid expansion to estimate cost savings for each tariff structure scenario, applied to a set of synthetic distribution feeders. Using this approach, we show how grid charging/discharging constraints enhance the distribution system cost savings from battery storage under standard TOU pricing structures, while also highlighting how better outcomes can be achieved with net billing or with refinements to TOU rate structures that better align charging and discharging profiles with times when it is most beneficial. This work focuses on evaluating policy options and their impact on distribution investments, rather than tariff design, which is the process by which specific rates are assigned to tariff structures and customer classes to achieve cost recovery in accordance with principles such as efficiency, cost causation, and fair compensation. The contributions of this paper are:

1. We developed a methodology to quantify and compare the impact of behind-the-meter battery adoption on distribution grid investments under different tariff schemes. The methodology combines tariff-driven battery operation policies with formal least-cost distribution grid expansion. To the authors' knowledge, this is the first application of such a detailed and integrated methodology in a large-scale policy study.
2. We use this methodology to perform a comparative analysis over 178 distribution feeders and 7 realistic scenarios of tariff-driven battery operation policies. We map tariff-driven battery operation to distribution grid costs and provide a decision-support framework for utilities to design DER incentive strategies that account for distribution grid infrastructure needs across current and future adoption scenarios.

2. Methodology and data

The methodology aims to determine the change in distribution grid investment costs when batteries, installed on feeders with high levels of PV and EV adoption, are operated in response to different tariff structures. Distribution grid investments under each tariff structure scenario are compared to grid investments under the corresponding *base case* with the same PV and EV assumptions, but no battery storage, in order to evaluate how battery operation impacts investments.

This section first describes the feeder data used in this analysis. We then summarize deployment-related assumptions for distributed PV, batteries, and EVs, including penetration levels, sizing, and load profiles. Next, we provide an overview of the tariff structures considered in the analysis. Finally, we provide an overview of the procedure for calculating distribution investments under each scenario. Further details on the investment model and calculations are provided in the Appendix section.

2.1. Feeder data

The analysis is conducted on a sample of 178 synthetic distribution feeders drawn from the larger SMART-DS dataset (Palmintier et al., 2020; Open Energy Data Initiative, 2020). The selected feeders are characterized by a predominant presence of residential consumers, which exhibit potential to trigger grid investments under PV adoption in the base scenario, i.e., with no batteries. It is important to note that the purpose of this paper is not to estimate absolute grid investments on these feeders. Instead, we use these feeders to compare grid investments relative to a base case with no batteries, assess how different tariffs affect battery operations, and then examine how this aggregate response leads to changes in distribution investments.

The hourly distribution of the selected feeders' peak load, before PV and batteries are added, is shown in Fig. 1. Most feeders' peak loads occur during the late afternoon and evening hours, with the greatest concentration at hour 19. Of the feeders studied in this analysis, 141 feeders have peak loads that occur during the TOU peak period (hours 17–22), while the remaining 37 feeders have peaks occurring in other, primarily early morning, hours. When discussing the results, the former group is referred to as *coincident feeders* while the latter is referred to as *non-coincident feeders*.

2.2. PV, EV, and storage assumptions

Key study assumptions for distributed PV, storage, and EVs are summarized in Table 1 and described in more detail below. These assumptions include the penetration rates for each technology, which are derived from existing literature and are intended to represent levels that might realistically be achieved across a utility's service territory under an aggressive 10-year growth trajectory (relative to present-day penetration rates in the U.S.). While higher penetration levels may be achieved in some areas or over longer time frames, the intent of this study was to select levels that would be broadly applicable to the near-term choices and decisions of utility resource planners today. The adoption rates selected for this analysis, consistent with the upper bound of NREL's Standard Scenarios, are intended to be sufficient to stress the distribution feeders and to capture the effect of each considered tariff on related distribution grid investments. Lower adoptions may limit the effect of batteries, reducing the impact on the resulting grid added/deferred costs.

PV penetration rates are assumed to reach 30% of all single-family residential buildings and 30% of all commercial load on each feeder, based on the upper bound scenarios from the National Renewable Energy Laboratory's recent set of Standard Scenarios (Gagnon et al., 2023). The feeder models used in this study do not identify specific dwelling types, and so all residential loads with a peak demand less than 20 kW are assumed to be a single-family home, and PV systems are randomly distributed across those loads until the specified penetration level is reached. Individual residential PV systems are sized to meet each home's total annual energy consumption, and nameplate ratings are derived using NREL's PVWatts model, based on solar radiation at the feeder location. The same sizing assumptions are used for each commercial PV system, which are randomly distributed across commercial loads on each feeder until the target penetration level is achieved.

Battery storage is assumed to be co-installed with 50% of all residential PV systems on each feeder. This assumption is based on a continued ramp-up in annual attachment rates from 28% of systems installed in 2024 (Solar Energy Industries Association, 2025). Battery

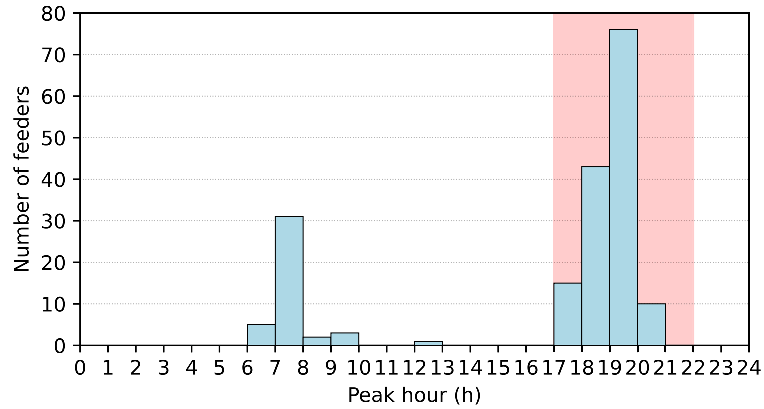

Fig. 1. Bar chart of peak occurrence times. The bars represent the number of feeders with a maximum load value occurring at the indicated hour. The highlighted area corresponds to the time-of-use peak price period.

Table 1
Key study assumptions for distributed PV, storage, and EVs.

Technology type	Penetration	Sizing	Load shape
Residential PV	30% of all single-family homes of each feeder	Sized to 100% of annual consumption for the individual site	Simulated with NREL PVWatts model for each feeder location using default inputs for panel orientation and losses
Commercial PV	30% of all commercial load on each feeder	Same as above	Same as above
Distributed storage	50% of all residential PV systems	Nearest increment of 5 kW to PV size and 2-hour duration	Simulated in response to tariff structure
Electric vehicles	50% of all single-family homes on each feeder	n/a	Selected from a set of 5000 unmanaged and 5000 managed charging profiles

sizing assumptions are based on current products and practices in the market today (Barbose et al., 2024). Batteries are sized such that the power rating is the largest multiple of 5 kW that is less than or equal to the PV system's capacity (but not less than 5 kW), and the energy storage capacity assumes a 2-hour duration battery, i.e., 2 kWh of energy storage per kW of power.

Finally, light-duty EV adoption is assumed to reach 50% of single-family homes (Wood et al., 2023). As with PV systems, EVs are randomly assigned across single-family homes on each feeder, regardless of whether PV or batteries are installed at the same location. While EV and PV could be correlated and affect the added/deferred cost analysis, the study focuses on determining the difference in added investments between each tariff case and a base case with no storage, to mitigate the effect of the base DER adoption. EV load profiles are based on a combination of managed and unmanaged charging profiles, assuming an even 50/50 split. For this purpose, a set of 5000 unmanaged and corresponding profiles are generated from a distribution of different combinations of EV types and models developed based on a recent NREL study (Wood et al., 2023) and using NREL's OCHRE model (Blonsky et al., 2021). To illustrate this approach, Fig. 2 provides examples of several unmanaged and the corresponding managed profiles for individual vehicles, along with the aggregate EV load profile for all EVs on a single feeder.

2.3. Tariff structure scenarios

Battery storage dispatch is simulated across a set of TOU-based tariff structures and net billing to show how each change in tariff structure incrementally impacts distribution system investments. The intent is not to identify the tariff structure that maximizes battery dispatch, but rather to compare performance across several known and readily implementable residential tariff structures. The tariff schemes considered include only the volumetric import/export components that affect battery response, then determine the related investments. While demand charges are relevant for incentivizing reductions in monthly peak demand, we are mainly focused on how hourly price signals under TOU and net billing affect battery operation and feeder investment needs.

All of the TOU-based tariff structures assume that the peak period is defined by the timing of peak demand and prices for the utility system as a whole, consistent with standard industry practice. To maintain internal consistency, those price forecasts are based on the same underlying market forecasts and the 10-year timeframe used for the distributed PV projections (Gagnon et al., 2023). For this study, TOU rates are assumed with a peak period from 5–10 p.m. (hours 17–22) on weekdays in each month. The specific prices are inconsequential, provided that the price differential between the highest- and lowest-priced TOU periods each day is large enough to offset round-trip efficiency losses and induce arbitrage cycling. Further details, including the mathematical formulation of each tariff, are included in Appendix A. The tariff structure scenarios considered in this study are summarized in Table 2. It is important to note that the tariffs used in this analysis are not designed endogenously to recover investment costs. Instead, these are treated as exogenous price signals that induce different charging and discharging responses. The process to specify how customers are charged to achieve cost recovery is outside the scope of this paper.

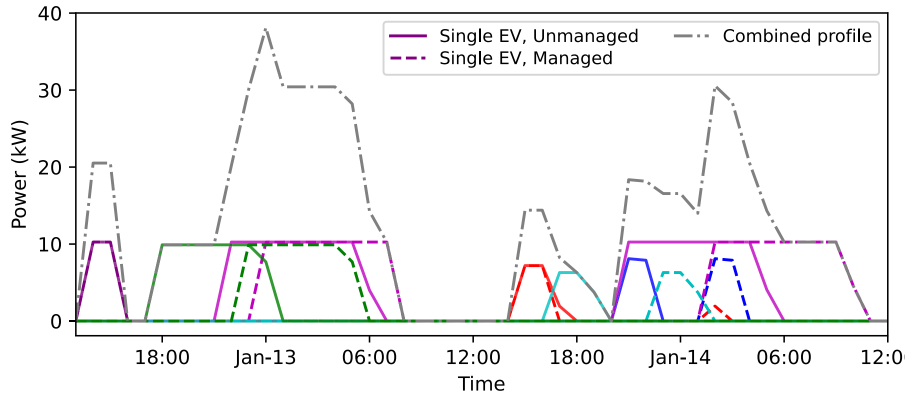

Fig. 2. Individual and combined managed and unmanaged EV profiles.

Table 2
Selected battery operation modes for evaluation.

Tariff scenarios	Charge strategy	Discharge strategy	Model in Appendix A
Unrestricted	Unrestricted	Unrestricted	$\beta = 1, \gamma = 1, k = 1$ tariffs as in (A.1)
Restrictive	Unrestricted	No grid discharge	$\gamma = 0, \beta = 1, k = 1$ tariffs as in (A.1)
	No grid charge	Unrestricted	$\beta = 0, \gamma = 1, k = 1$ tariffs as in (A.1)
	No grid charge	No grid discharge	$\gamma = 0, \beta = 0, k = 1$ tariffs as in (A.1)
Incentivized	Super off-peak charge	No grid discharge	$\gamma = 0, \beta = 1, k = 1$ tariffs as in (A.2)
	No grid charge	Over-the-peak discharge	$\beta = 0, k = 2/5, \gamma = 1$ tariffs as in (A.1)
	Super off-peak charge	Over-the-peak discharge	$\beta = 1, k = 2/5, \gamma = 1$ tariffs as in (A.2)
	Net billing	Net billing	$\beta = 1, \gamma = 1, k = 1$ tariffs as in (A.3)

2.4. Computation of net loads and distribution investment impacts

Here we provide a high-level overview of the computational methods used to quantify the impacts of battery storage operation on distribution system investments, with further details contained in the appendix, illustrated in Fig. 3. Each feeder consists of a collection of individual customer loads, a subset of which are outfitted with PV and battery storage, per the adoption assumptions outlined earlier. For each tariff structure scenario, the analysis sequence begins by computing the hourly net load for each PV+storage customer on each feeder, optimizing storage dispatch based on the customer's net demand and the specific tariff characteristics of the scenario under study. The model for calculating net load is described in detail in Appendix A, which is parameterized according to Table 2 according to the tariff structure to evaluate. The battery operation optimization assumes that all customers operate their batteries to perfectly minimize operating costs. While behavioral factors or imperfect information may affect battery operation, this solution enables evaluation of conditions in which battery charging/discharging coincide, potentially causing severe stress on the distribution grid. The effect of battery degradation is neglected in this study, as the evaluation is conducted over a one-year window. Next, planning days for each feeder are selected, consisting of the maximum, minimum, and average demand days, obtained from the net loads aggregated at the feeder head level. The selection of planning days is outlined in Appendix B. Finally, we use Berkeley Lab's LODGE model, a distribution system expansion model, to compute upgrade costs on each feeder under each tariff scenario, based on the corresponding set of planning days, as described further in Appendix C. It is important to note that the selection of these days aims to represent stress conditions on the distribution feeders. Since operation costs are not involved in LODGE objective function, these are equally weighted for the investment optimization. Those costs are ultimately expressed on an annualized basis and compared to the annualized upgrade costs under the base case with no storage.

2.5. Evaluation metric

To compare and aggregate results across feeders in the sample, we normalize the annualized investment for each feeder by its installed battery capacity. Investment impacts are thus denominated in terms of added/deferred cost ($) per kW of storage (kW$_S$). Note that this analysis focuses on investment optimization, considering only the utility-level benefits of the resulting battery dispatch under each tariff structure.

The total annualized investment cost for feeder f in tariff structure c, I_{fc}, is obtained from combining the annualized line reconductoring (IC^{rc}_{fc}), transformer upgrading (IC^{tr}_{fc}), and voltage regulator investments (IC^{vr}_{fc}) obtained for feeder f and tariff structure c from the expansion planning model evaluation in Appendix C,

$$I_{fc} = IC^{rc}_{fc} + IC^{tr}_{fc} + IC^{vr}_{fc}, \qquad \forall f, \forall c. \tag{1}$$

Finally, the metric is obtained for each feeder f and tariff structure c, as,

$$m_{fc} = \frac{I_{fc} - I_{f,base}}{\sum\limits_{\forall h} \overline{p^{\text{batt}}_{fh}}}, \qquad c \in C, \forall f, \tag{2}$$

where $I_{f,base}$ is the annualized investment for feeder f considering the base case with no battery operation. Positive values of m_{fc} indicate

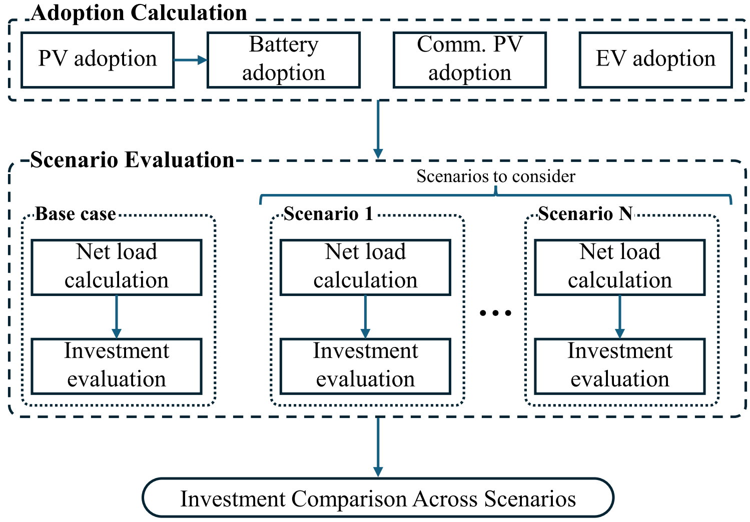

Fig. 3. Methodology to assess the impact of different battery operation modes on distribution grid investments for a given distribution feeder. The base case corresponds to the scenario where grid investments are obtained when no battery operation is considered, while the remaining scenarios refer to considered alternatives for battery operation.

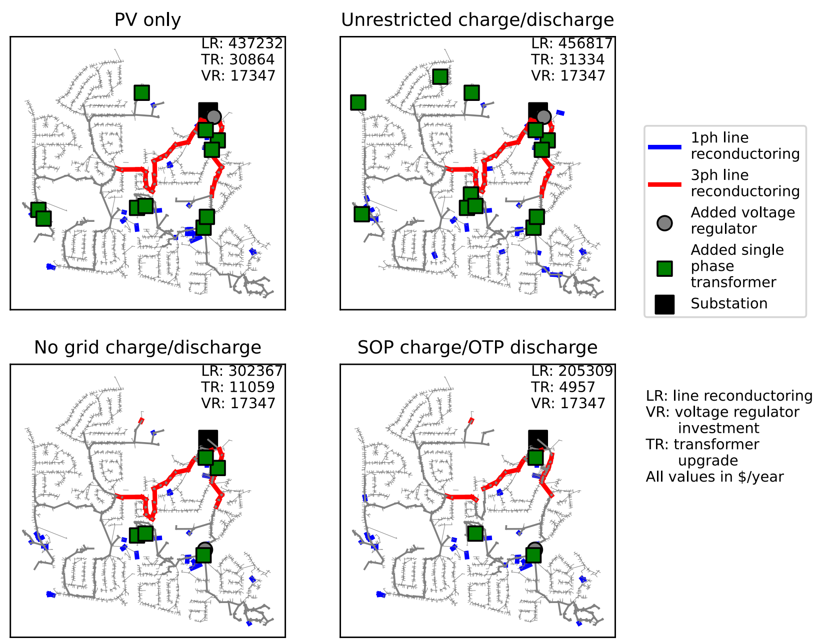

Fig. 4. Investment placement under different tariff scenarios.

increased investment costs for f under scenario c, while negative values indicate investment deferrals when batteries are operated under tariff structure c.

3. Results and discussion

Our primary results focus on a base case with high distributed PV adoption, without yet adding high EV adoption. The rationale for this approach is that residential battery storage adoption has almost exclusively occurred in conjunction with PV adoption, hence the need to understand the interactions between these two technologies specifically. To build intuition, Section 3.1 illustrates the upgrades and associated cost impacts for a single feeder, under the base case and a subset of the tariff scenarios. Section 3.2 then presents the core set of results across all feeders and tariff scenarios. Sections 3.3 to 3.5 describe in more detail the results for each set of tariff scenarios, linking the investment impacts to the underlying battery dispatch profile, and also highlighting important sources of variation across feeders in the sample. Finally, Section 3.6 presents the results of the sensitivity analysis with high EV loads added, showing how the investment impacts under each tariff scenario are altered as a result of the additional loads.

3.1. Investment impacts for single feeder example

We begin by illustrating the investment impacts for a single feeder from the SMART-DS dataset, with a 18,412 kW peak demand, 17,322 kW of combined residential and commercial solar, and 4495 kW of installed battery storage. Investment results for the PV-only base case in Fig. 4 show multiple additions to address issues arising from base conditions and the added solar capacity. These additions include single-phase transformer upgrading, reconductoring of three-phase and single-phase line sections, and installation of a voltage regulator close

Table 3
Annualized investment costs and added/deferred costs per kW of installed storage for feeder p5uhs22_1247–p5udt9433.

Scenario	Total investment ($/year)	Difference with respect to base case ($/year)	Added/deferred costs per kW of storage (m_{fc}, $/kW$_S$-year)
PV only (Base case)	485,443	–	–
PV+battery (Unrestricted charge/discharge)	505,498	+20,055	+4.46
PV+battery (No grid charge/discharge)	330,773	–154,670	–34.41
PV+battery (SOP charge/OTP discharge)	227,613	–257,830	–57.36

Table 4
Number of feeders with every investment outcome for each strategy (n = 178)

Battery operation mode	Coincident Peak (n = 141)			Non-coincident Peak (n = 37)		
	Neutral invest.	Deferred invest.	Increased invest.	Neutral invest.	Deferred invest.	Increased invest.
Unrestricted charge/discharge	48	60	33	32	2	3
Restricted discharge	23	79	39	33	1	3
Restricted charge	27	95	19	21	12	4
Restricted charge/discharge	10	112	19	30	5	2
Restricted charge/OTP discharge	5	125	11	20	15	2
SOP charge/Restricted discharge	5	121	15	11	22	4
SOP charge/OTP discharge	3	123	15	17	16	4
Net billing	8	116	17	10	25	2

Table 5
Comparison of peak load variation and battery usage across considered tariffs.

			Unrestricted charge/discharge	No grid discharge	No grid charge	No grid charge/discharge	No grid charge/OTP discharge	SOP charge/No grid discharge	SOP charge/OTP discharge	Net billing
Max. net load day	Average max. peak reduction (kW/kW$_S$)	Coinc.	−0.13	−0.22	−0.14	−0.29	−0.34	−0.27	−0.34	−0.32
		Non-coinc.	0.03	0.02	0.00	0.00	0.00	−0.04	0.06	−0.06
		Overall	−0.10	−0.17	−0.11	−0.23	−0.27	−0.23	−0.25	−0.26
	Average batt. discharge (kWh/kW$_S$)	Coinc.	2.00	1.35	1.57	1.20	1.61	2.02	2.00	1.88
		Non-coinc.	2.00	0.96	1.25	0.82	1.25	1.72	2.00	1.32
		Overall	2.00	1.26	1.51	1.12	1.53	1.96	2.00	1.76
Min. net load day	Average min. load increase (kW/kW$_S$)	Coinc.	0.00	0.00	0.29	0.02	0.29	0.29	0.43	0.29
		Non-coinc.	0.00	0.00	0.23	0.01	0.23	0.17	0.46	0.24
		Overall	0.00	0.00	0.28	0.02	0.28	0.26	0.43	0.28
	Average batt. charge (kWh/kW$_S$)	Coinc.	2.00	0.80	1.99	0.91	1.99	1.64	2.00	2.00
		Non-coinc.	2.00	0.69	2.00	0.82	2.00	1.42	2.00	2.00
		Overall	2.00	0.78	1.99	0.89	1.99	1.60	2.00	2.00

to the substation for voltage control. Based on the cost assumptions in (1)–(2), network upgrades in the base case amount to an annualized investment cost of $485,443, as shown in Table 3. When batteries are included and operated without restrictions, upgrade costs are increased by $20,055/year compared to the base case — an added $4.46/kW$_S$ — due to additional line and transformer upgrades. If the batteries are instead operated in a fully restricted mode with no grid charge or discharge allowed, less line reconductoring and considerably fewer transformers upgrades are required, leading to an estimated deferral value of $34.41/kW$_S$. Finally, battery operation under the incentivized tariff scenario that combines super off-peak charge and over-the-peak discharge further reduces the need for network upgrades, leading to deferral value of $57.36/kW$_S$.

3.2. Investment impacts across full feeder sample

Fig. 5 summarizes the results for all feeders and tariff scenarios in terms of the change in investment costs compared to the PV-only base case. The figure presents the distribution across all feeders for each tariff scenario, distinguishing between feeders with peak loads that are either coincident or non-coincident with the TOU peak period. Table 4 provides some additional detail by showing the number of feeders with either increased, decreased, or no change in investment costs under each tariff scenario.

Several key findings emerge from these comparisons. First, across all of the tariff scenarios analyzed, the net investment impacts on any individual feeder may be positive (added costs), negative (deferred or avoided costs), or neutral (no change in costs). Second and related, the changes in investment costs are most pronounced for coincident feeders. In comparison, the majority of non-coincident feeders exhibit no change in investment costs in most of the tariff scenarios, and when deferrals do occur, they are generally much smaller than those on coincident feeders. This suggests that feeders with morning peaks could be subject to a different tariff design better aligned with their peak times to improve efficiency and reduce costs for customers. In these cases, a net billing scheme is more beneficial for this purpose compared to TOU. Finally, deferrals increase substantially from the unrestricted case to the fully restricted case with no grid charging or discharging,

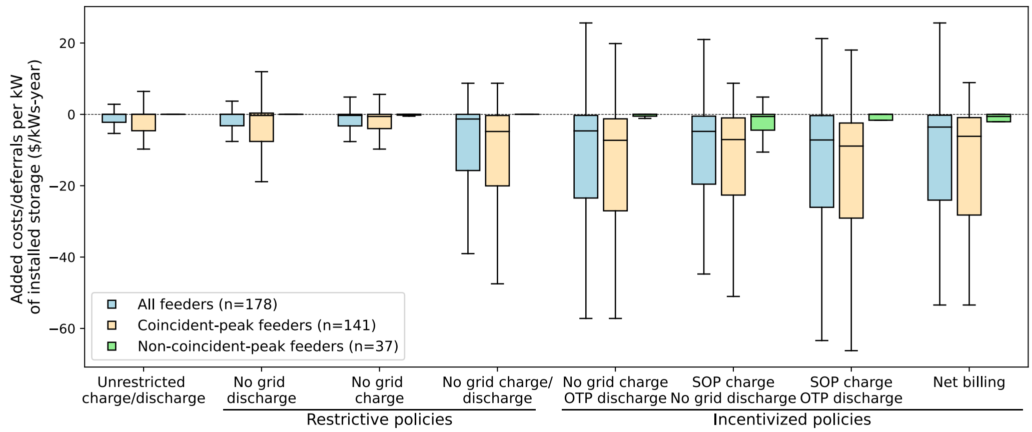

Fig. 5. Added cost distribution per kW of installed storage across tariffs, including distribution of coincident, non-coincident, and all feeders. This box-and-whiskers chart includes median, first and third quartile.

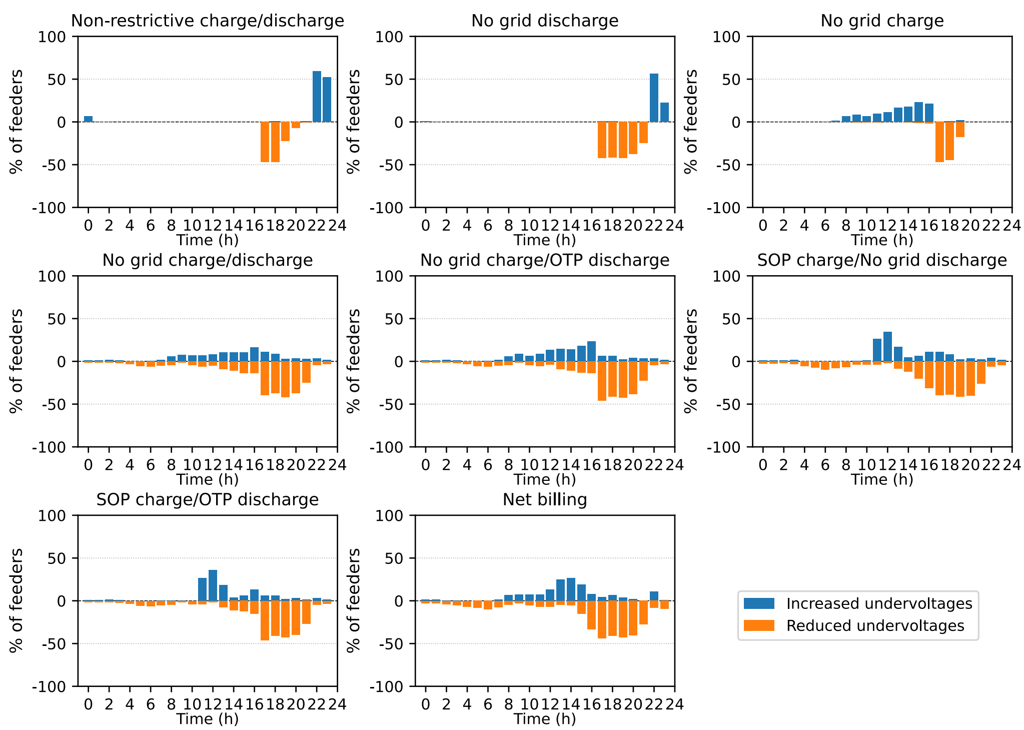

Fig. 6. Percentage of feeders with added and reduced undervoltages at each hour for each tariff compared to the PV-only scenario.

and then increase modestly more when moving to the incentivized cases. Differences across the incentivized cases are relatively small, but the largest deferral values occur for the tariff that combines a super off-peak TOU rate (SOP) with rules that require even discharge over the peak TOU period (OTP).

Battery dispatch profiles under each tariff scenario differ in terms of both the timing and quantity (i.e., cycle depth) of energy charged/ discharged. The findings above are driven to a significant degree by the resulting changes in peak and minimum load across feeders in the sample (see Table 5), and the corresponding change in the prevalence of voltage violations (see Figs. 6 and 7). Voltage violations are a key concern in this study, as distribution grid voltages are required to remain within ±5% of the feeder rated voltage in normal operating conditions. The next set of sections further describe the results under each tariff structure, explaining the investment impacts in terms of the underlying battery storage dispatch profile and differences across feeders in the sample.

3.3. The reduced potential from unrestricted grid charging and discharging

The charging cycle under this tariff structure is fundamentally misaligned with the timing of minimum and maximum load on most feeders, as storage charging and discharging both occur as soon, as quickly, and as fully as possible at the beginning of the TOU off-peak and peak periods, respectively. Hence, the unrestricted battery operation provides no benefit in addressing overvoltage issues at times of high PV generation. In addition, the rapid and synchronized charging at the start of the off-peak period can shift the feeder peak to those hours, increasing the peak net load as shown in Fig. 8-b. On the other hand, peak load reductions may occur on feeders with narrow peak loads coinciding with battery discharge during the first few hours of the TOU peak period, as shown in Fig. 8-a. A separate issue can also occur during the discharge cycle if high PV exports are also occurring during those hours, leading to more overvoltage violations in the initial peak period hours (see Fig. 7). Compared to the incentivized tariff structures, nearly 50% fewer feeders report investment deferrals, while the number

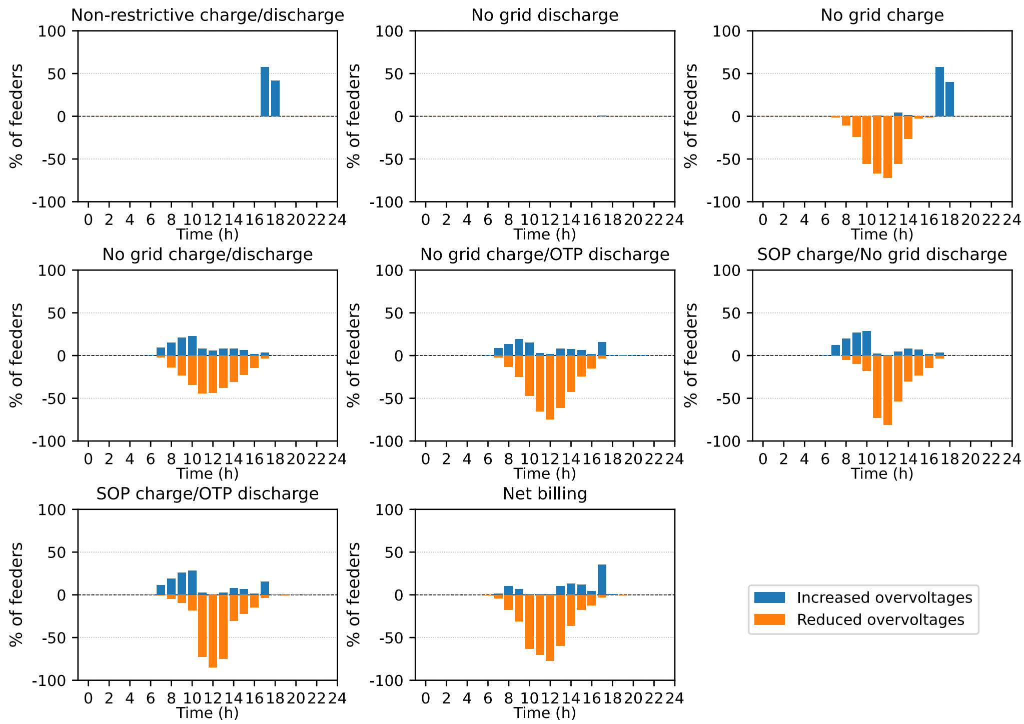

Fig. 7. Percentage of feeders with added and reduced overvoltages at each hour for each tariff compared to the PV-only scenario.

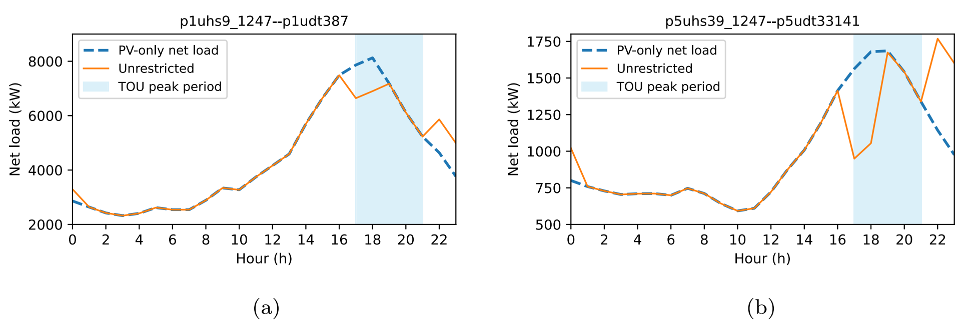

Fig. 8. Net load profile comparison between the scenario with no battery and the scenario with unrestricted battery charge/discharge (a) feeder where the maximum net load is reduced, (b) feeder where the maximum net load is shifted and increased.

of feeders with added investments is doubled, indicating a significant reduction in the potential benefits of battery integration. Regarding impacts on costs, they are generally small, with an inter-quartile range of -\$4.59 (savings) to \$0/kW$_S$-year (Fig. 5).

3.4. Restricting grid charging and discharging

Restrictions on grid charging and discharging shift the timing of storage charging and discharging (see Fig. 9-a and 9-b), aligning it more closely with grid needs, though these benefits can be muted by reductions in storage cycling depth. As a result, restrictions on grid charging and discharging each lead to modest gains in deferral value when implemented individually, but greater gains when implemented together.

In the No Grid Discharge scenario, the discharge energy is spread more evenly across the TOU peak period, compared to the unrestricted case, as shown in Fig. 9-a. The battery discharge is reduced about 32.5% across coincident-peak feeders, as battery only discharge to meet net consumer load during the TOU peak. Compared to the base case, larger average peak load reductions (0.22 vs. 0.13 kW/kW$_S$) and more frequent reductions in undervoltages across a larger range of hours (Fig. 6) occur compared to the base case.

On the other hand, in the No Grid Charge scenario, restrictions on grid charging shift the charging load from the early evening hours of the TOU off-peak period to daytime hours when PV surplus is available, as shown in Fig. 9. The impact is twofold: first, it eliminates the charging peak during early off-peak hours when feeder loads are still relatively high, and second, it aligns better storage charging with minimum load conditions during times of high PV grid injections. Shifting charging to those times results in an average increase in minimum feeder load of 0.29 kW/kW$_S$ (compared to 0 in the unrestricted case), and a substantial reduction in the frequency of overvoltage violations during those midday hours (Fig. 7). As a result of these shifts in the timing of storage charging, net cost savings occur on a substantially higher fraction of feeders—including both coincident-peak and non-coincident-peak feeders (see Table 4).

Combining the grid charging and discharging restrictions leads to greater peak load reductions than from either restriction alone, and more than double the level in the unrestricted case (Table 5). However, the grid discharge restriction also reduces the depth of discharge and thus the amount of charging, which diminishes the ability to address overvoltage violations from high levels of PV grid injections on minimum load days. This is evident by comparing the minimum-load-day metrics in Table 5, which shows only a negligible increase in

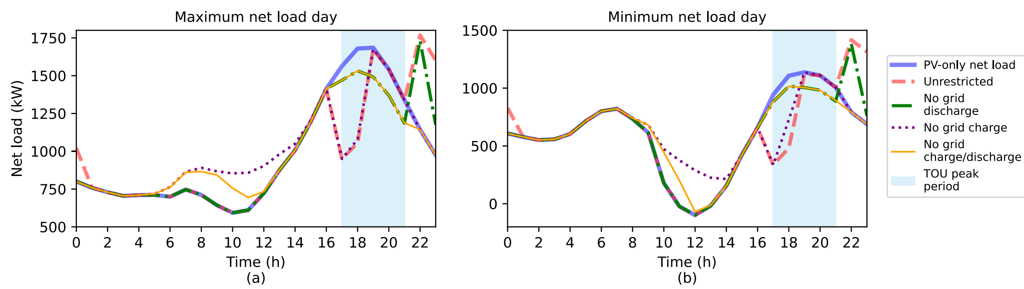

Fig. 9. Comparison between net load profile under restricted battery operation modes (a) maximum net load day, (b) minimum net load day.

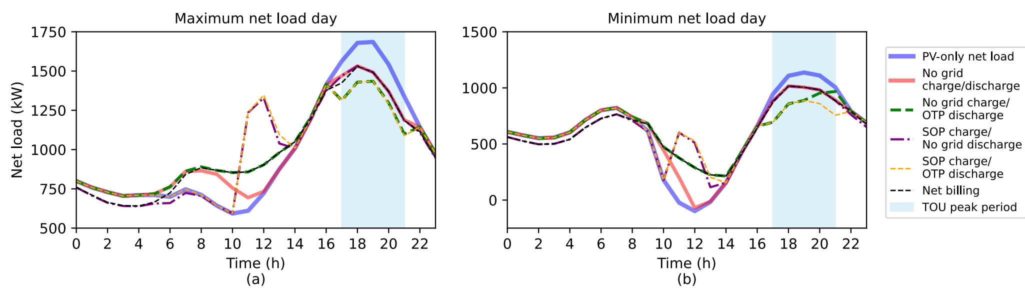

Fig. 10. Comparison between net load profile under incentivized battery operation modes (a) maximum net load day, (b) minimum net load day.

average minimum load in this scenario, and can also be seen visually in the example shown in Fig. 9-b. On net, however, the greater peak load reductions in this scenario prove more consequential, leading to substantially greater deferral values under this scenarios for coincident feeders, compared to the cases with just one or another restriction.

3.5. The benefits of incentivized battery operation

While the grid charging/discharging restrictions presented in the previous section generally improve investment outcomes relative to the unrestricted case, they also tend to constrain cycling depth limiting the potential benefits from deferral distribution system upgrades. The changes in battery dispatch profile under each of these incentivized tariff structures is illustrated in Fig. 10, for one individual feeder. Below, we describe the resulting impacts on distribution feeder investment costs across the full sample of feeders.

OTP discharge distributes the discharge energy evenly across the TOU peak period, leading to substantially larger peak reductions than in the fully restricted case (0.34 vs. 0.29 kW/kW$_S$, as shown in Table 5). In addition, by allowing full discharge, OTP discharge significantly increases charging demand on minimum load days, boosting the ability of the battery to address overvoltage issues from high PV grid injections, as seen by comparing the minimum-load-day metrics in Table 5 and net load profiles in Fig. 10-b. As a result, replacing the grid charging restriction with OTP discharge increases the median deferral value across all feeders in the sample from \$1.30/kW$_S$ to \$4.64/kW$_S$, more than a three-fold increase.

Shifting to incentivized charging, the ability of SOP charging to shift the storage charging to occur during midday hours provides modest peak load reductions on non-coincident-peak feeders. More importantly, it allows for more complete discharging and thus more midday charging to help address problems associated with high levels of PV grid injections, compared to the fully restricted case and the case with SOP charging and no grid discharge (Table 5). This operation has two key limitations. First, the tariff fails to address overvoltage issues during adjacent hours, shifting minimum load to those hours. Second, the aggregated charging can create sharp peaks that potentially diminish or offset load reductions during the TOU peak period.

Combining SOP charging with OTP discharging produces a similar battery dispatch profile to SOP charging with no grid discharge, but with complete charging and discharging each cycle. This case yields by far the largest increase in average minimum load across the feeder sample (0.43 kW/kW$_S$, as shown in Table 5). Among coincident-peak feeders, however, peak load reductions are the greatest of any of the scenarios evaluated. On net, this scenario yields the largest median deferral value across any of the tariff scenarios evaluated (\$7.18/kW$_S$, across all feeders in the sample), given the combination of relatively large peak load reductions on coincident feeders and, by far, the largest increases in minimum load across all feeders.

Net billing, on the other hand, enables and incentivizes batteries to discharge to meet customer load throughout nighttime hours beyond the end of the TOU peak period. As a result, the charging profile under net billing is more evenly distributed across daytime hours. In terms of peak load impacts, the net billing case leads to among the largest reductions of the tariffs analyzed, though slightly lower than the OTP discharge cases for coincident feeders (0.32 vs. 0.34 kW/kW$_S$), given the constraint on battery discharge to only serve residual net load. For that reason and the smaller impact on minimum load, the median deferral value in the net billing case is well below the value in the OTP discharging/SOP charging case (\$3.56 vs. \$7.18/kW$_S$, as shown in Fig. 5).

3.6. Sensitivity with high EV loads

The scenario analysis presented in this section adds high EV adoption to evaluate how EV integration impacts the investment deferral value of battery storage. Note that PV and battery sizing is held constant between the primary analysis and the high EV sensitivity, that EV loads consist of a combination of managed and unmanaged EV load profiles, and that its operation is not responsive to changes in the tariff structure. As shown in Fig. 11, the additional EV loads increase feeder net load across all hours. The resulting impacts on upgrade costs are summarized in Fig. 12, which compares the change in distribution system investment costs under each tariff structure scenario with respect to the corresponding base case, for both the primary analysis with no EV load and the sensitivity analysis with added EV loads.

In general, the added EV load tends to diminish slightly the ability of battery storage to reduce distribution system upgrade costs, as can be seen by the upward shift in the cost distributions for all of the tariff scenarios shown in Fig. 12. This occurs mainly because the added

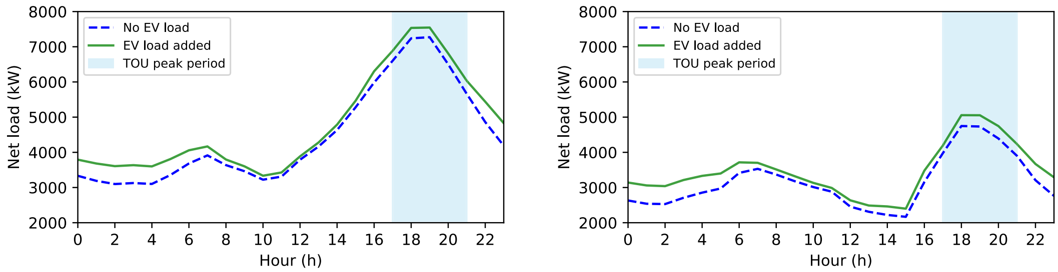

(a)

(b)

Fig. 11. Comparison between net load profiles with and without EV loads: (a) Maximum net load day, (b) minimum net load day.

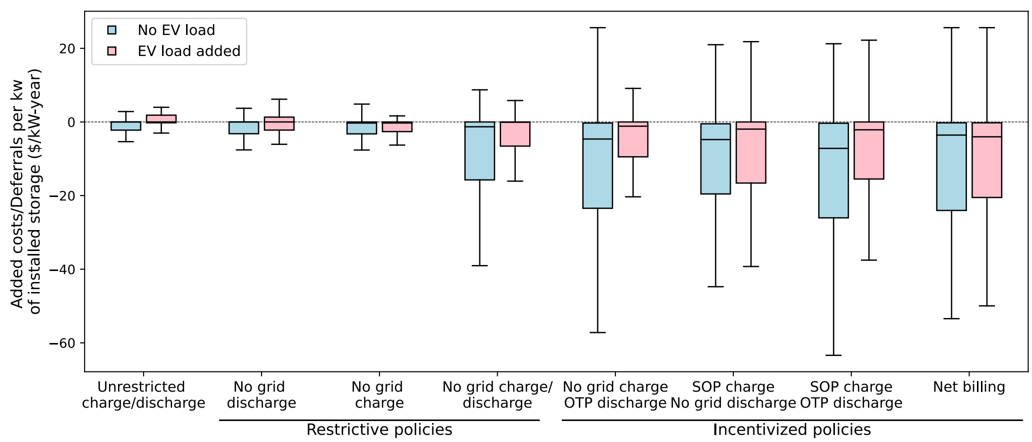

Fig. 12. Added/deferred investment distribution per kW of installed storage across tariffs. Distribution when EV loads are considered is included for comparison.

Table 6

Distribution of feeders with added/neutral/deferred investments for each tariff and the effect of EV loads.

	w/o EV loads (%)			with EV (%)		
	Deferred	Neutral	Increased	Deferred	Neutral	Increased
Non-restrictive charge/discharge	34.8	44.9	20.2	28.8	37.3	33.9
No grid discharge	44.9	31.5	23.6	36.2	29.4	34.5
No grid charge	60.1	27.0	12.9	59.3	31.1	9.6
No grid charge/ discharge	65.7	22.5	11.8	50.3	39.5	10.2
No grid charge/ OTP discharge	78.7	14.0	7.3	66.1	24.3	9.6
SOP charge/No grid discharge	80.3	9.0	10.7	72.9	11.3	15.8
SOP charge/ OTP discharge	78.1	11.2	10.7	73.4	13.6	13.0
Net billing	79.2	10.1	10.7	76.8	12.4	10.7

EV loads amplify any negative impacts associated with the battery storage charging peaks. These effects occur primarily on non-coincident feeders, where battery storage leads to greater increases in feeder peak loads in the EV sensitivity case, compared to the core set of cases without EV loads. As a result, in the EV sensitivity, a smaller percentage of feeders see net deferrals in each tariff scenario, and in many (though not all) tariff scenarios, a larger percentage of feeders see a net increase in investment costs (see Table 6).

4. Conclusion and policy implications

Rapid growth of distributed PV and EVs may require significant upgrades to distribution networks, but distributed battery storage can help to defer or avoid those upgrades, depending on how it is operated. This study examines how tariff structures in place today — namely TOU rates and net billing tariffs — can induce storage operations that help defer distribution upgrade costs associated with high levels of PV and EVs. TOU rates with unrestricted grid charging and discharging generally yield little deferral value, and on some feeders, may even increase upgrade costs. Restricting grid charging and discharging produces greater deferrals and fewer cost increases, but limits battery cycling depth constraining potential benefits. The incentivized TOU tariff structures analyzed in this study enable fuller utilization of battery capacity and further improve outcomes relative to TOU rates with no grid charging or discharging. The net billing tariff, which is an increasingly common U.S. pricing structure, produces deferral value similar to that of incentivized TOU structures. Finally, high EV adoption erodes storage deferral value across all tariff structures considered, largely due to the compounding effects of greater EV load combined with storage charging.

Several key implications emerge from these findings. First and foremost, existing tariff structures, in the form of TOU rates and net billing, can be used to effectively mobilize battery storage to reduce distribution upgrade costs associated with increased distributed PV and EVs, but the value is highly dependent on specific features of the tariff structure. Moreover, those deferral benefits are largely confined to feeders whose peak loads coincide with the broader utility system peak (and hence with the timing of the TOU peak period). Capturing deferral value on non-coincident feeders may require more location-specific pricing structures or program designs that induce storage discharge that coincides with the individual feeder peak. Even for coincident-peak feeders, the TOU structures analyzed in this study are likely far from optimal for maximizing the value of storage deferral. For example, the best-performing tariff structures yielded an average peak demand reduction of 0.34 kW/kW_S across the peak-coincident feeders, and an average increase in minimum load of 0.43 kW/kW_S (compared to an ideal maximum of 1.00 kW/kW_S). Other refinements to TOU-based designs could no doubt yield incremental improvements, though more locationally specific and dynamic tariff or program designs would likely be needed to realize substantially greater benefits. Finally, the analysis of the PV+EV scenarios indicated that the ability of battery storage to defer grid investments diminishes with load growth when the new load is inflexible.

Future work should evaluate the sensitivity of the obtained results to battery duration. While this study considered batteries with a 2-hour capacity given current market practices, the effect of the additional battery capacity varies depending on the evaluated tariff and operating strategy. Under unrestricted operation, the charging and discharging periods are extended. However, because battery power output remains constant, the stress on the distribution grid is concentrated during the first hours of the TOU peak and off-peak periods. In contrast, the super-off-peak charge may lead to overnight charging if the required charging time exceeds the SOP period, potentially increasing investment compared to unrestricted operation. As for net billing, the additional battery capacity allows extra charging and additional discharge during TOU off-peak periods. Future studies should also evaluate how more refined forms of managed EV charging or other flexible loads can improve deferrals of grid upgrades. In addition, future work could consider the effects of monthly demand charges and how battery operation can also shift the maximum customer demand.

CRediT authorship contribution statement

Luis Rodriguez-Garcia: Writing – review & editing, Writing – original draft, Visualization, Validation, Software, Methodology, Formal analysis, Data curation. **Galen Barbose:** Writing – review & editing, Writing – original draft, Validation, Supervision, Methodology, Funding acquisition, Conceptualization. **Sydney Forrester:** Writing – review & editing, Writing – original draft, Methodology, Conceptualization. **Michael Blonsky:** Writing – review & editing, Writing – original draft, Software, Methodology, Data curation, Conceptualization. **Miguel Heleno:** Writing – review & editing, Writing – original draft, Supervision, Resources, Project administration, Methodology, Formal analysis, Conceptualization.

Declaration of competing interest

The authors declare that they have no known competing financial interests or personal relationships that could have appeared to influence the work reported in this paper.

Acknowledgments

The work described in this study was funded by the U.S. Department of Energy's Office of Energy Efficiency and Renewable Energy under Lawrence Berkeley National Laboratory Contract No. DE-AC02-05CH11231.

Appendix A. Battery dispatch and net load calculation

This Appendix first discusses the rationale for the tariff structures considered in this study. Then, it presents the mathematical formulation for evaluating each tariff structure. Finally, the optimization model for calculating the net load at the grid connection point of each single-family home with PV and batteries, given a tariff structure, is formulated.

A.1. Tariff categories based on battery operation restrictions

A.1.1. Unrestricted scenario

The unrestricted tariff structure is a two-period TOU rate with no restrictions on grid charging or discharging. Battery dispatch under this scenario is triggered by changes in electricity prices and is limited only by the battery capacity. As a result, all batteries charge as quickly as possible (within two hours) after the start of each TOU off-peak period, and discharge as quickly as possible after the start of each TOU peak period. This scenario maximizes energy arbitrage between peak and off-periods, subject only to the battery size and its stipulated minimum state-of-charge limit.

A.1.2. Restrictive scenarios

The next set of tariff structure scenarios explores prohibiting grid charging, grid discharging, or both, all layered onto the same TOU rate as the unrestricted scenario. Under the *no grid charge* cases, batteries can only be charged from PV generation in excess of load during each hour. This serves to delay charging until daytime hours and limit the rate of charging to amount the surplus PV generation in each hour, rather than allowing the battery to fully charge after the off-peak rate begins each evening. If insufficient surplus solar is available during off-peak hours on any given day, the battery may not fully charge, which may then also limit the volume of energy discharged. Under the *no grid discharge* cases, batteries only discharge to meet the residual load not supplied by PV generation during each TOU peak period. This serves to reduce the rate of discharge based on the amount of residual load in any given hour. If insufficient residual load is available during peak period hours on any given day, the battery may not fully discharge to its minimum limit, which may then also limit the volume of charging.

A.1.3. Incentivized scenarios

The preceding set of restricted cases aims to mitigate potential issues from unrestricted grid charging and discharging, but does so bluntly by prohibiting any level of grid charging or discharging. Those restrictions will tend to suppress cycling depth for the reasons noted above, thereby dampening the ability of the battery to mitigate grid stresses associated with distributed PV and EVs. They also fail to redirect the charging or discharging to times when it would be more beneficial. This group of tariffs aim to either shift or smooth the charging and discharging, rather than imposing hard constraints on grid charging or discharging that reduce the cycling depth, by substituting one or more of the following features:

- **Super off-peak (SOP) charge:** A third TOU period with even lower, super-off-peak prices is added on weekdays from 10 a.m.–1 p.m., to shift battery charging to the hours where the greatest amounts of surplus PV generation are expected.

- **Over-the-peak (OTP) discharge:** Batteries are required to be discharged at a continuous rate over the whole duration of the TOU peak period, rather than discharging as quickly as possible at the beginning of the period.
- **Net billing:** Consumers are disincentivized but not prohibited from grid discharging and grid charging by significantly reducing the export tariff compared to the import rate.

In total, four *Incentivized* tariff structure scenarios are created by substituting grid charging and/or discharging restrictions in the fully restricted case with one or more of the features above.

A.2. Tariff structure formulation

Three sets of tariff structures are considered for evaluation: Time-of-Use (TOU), Time-of-Use plus a super-off-peak period, and net billing. The TOU structure is considered for the cases not involving super-off-peak charge or net billing, and is defined as:

$$\lambda_t^{\text{imp}} = \lambda_t^{\text{exp}} = \begin{cases} \lambda^{\text{peak}}, & t \in \mathcal{T}^{\text{peak}}, \\ \lambda^{\text{offpeak}}, & t \in \mathcal{T}^{\text{offpeak}}, \end{cases} \tag{A.1}$$

where $\lambda_t^{\text{imp}}, \lambda_t^{\text{exp}}$ are the unit cost of energy consumed and energy exported, respectively, λ^{peak} is the unit cost during peak hours $\mathcal{T}^{\text{peak}}$, λ^{offpeak} is the unit cost during off-peak hours $\mathcal{T}^{\text{offpeak}}$, $\lambda^{\text{offpeak}} < \lambda^{\text{peak}}$. An alternative to incentivize charging during times of excessive solar generation is allowing a period during morning hours where charging is cheaper (super-off-peak period), described as

$$\lambda_t^{\text{imp}} = \lambda_t^{\text{exp}} = \begin{cases} \lambda^{\text{peak}}, & t \in \mathcal{T}^{\text{peak}}, \\ \lambda^{\text{offpeak}}, & t \in \mathcal{T}^{\text{offpeak}}, \\ \lambda^{\text{super}}, & t \in \mathcal{T}^{\text{super}}, \end{cases} \tag{A.2}$$

where λ^{super} is the unit cost during the super-off-peak period $\mathcal{T}^{\text{super}}$, where $\lambda^{\text{super}} < \lambda^{\text{offpeak}} < \lambda^{\text{peak}}$. Finally, another structure considered for this study is net billing. In this case, different rates are applied to imported and exported energy, as follows

$$\lambda_t^{x} = \begin{cases} \lambda^{\text{peak,x}}, & t \in \mathcal{T}^{\text{peak}}, \\ \lambda^{\text{offpeak,x}}, & t \in \mathcal{T}^{\text{offpeak}}, \end{cases} \quad x = \{\text{imp}, \text{exp}\}, \tag{A.3}$$

where $\lambda^{\text{peak,exp}}, \lambda^{\text{offpeak,exp}}$ are the exporting rates during peak and off-peak periods, respectively, and $\lambda^{\text{peak,imp}}, \lambda^{\text{offpeak,imp}}$ are the importing rates during peak and off-peak periods, respectively, and $\lambda^{\text{offpeak,exp}} < \lambda^{\text{peak,exp}} < \lambda^{\text{offpeak,imp}} < \lambda^{\text{peak,imp}}$.

A.3. Mathematical model for battery dispatch and net load calculation

Let $\mathcal{F} = \{1, \dots, F\}$ define the set of feeders, $C = \{1, \dots, C\}$ define the set of battery operation scenarios, $\mathcal{H} = \{1, \dots, H\}$ define the set of single-family homes, and $\mathcal{T} = \{1, \dots, T\}$ define the set of time steps. The battery dispatch is calculated with the model presented in (A.4)–(A.19) over one year (8760 hourly samples), where constraints are defined for all t, policy c, and all homes h connected to feeder f, except where indicated.

$$\min \sum_{t \in \mathcal{T}} \left(\lambda_t^{\text{imp}} p_{fcht}^{\text{imp}} - \lambda_t^{\text{exp}} p_{fcht}^{\text{exp}} \right), \tag{A.4}$$

s.t.,

$$p_{fcht}^{g-l} + p_{fcht}^{s-l} = p_{fcht}^{l+}, \tag{A.5}$$

$$p_{fcht}^{p-g} + p_{fcht}^{p-s} = -p_{fcht}^{l-}, \tag{A.6}$$

$$p_{fcht}^{l+} = \max\{p_{fcht}^{load} - p_{fcht}^{pv}, 0\}, \tag{A.7}$$

$$p_{fcht}^{l-} = \min\{p_{fcht}^{load} - p_{fcht}^{pv}, 0\}, \tag{A.8}$$

$$p_{fcht}^{\text{imp}} - p_{fcht}^{\text{exp}} = p_{fcht}^{g-s} + p_{fcht}^{g-l} - p_{fcht}^{s-g} - p_{fcht}^{p-g}, \tag{A.9}$$

$$0 \le p_{fcht}^{g-s} + p_{fcht}^{p-s} \le \overline{p_{fh}^{\text{batt}}}, \tag{A.10}$$

$$0 \le p_{fcht}^{s-g} + p_{fcht}^{s-l} \le k\, \overline{p_{fh}^{\text{batt}}}, \tag{A.11}$$

$$E_{fcht} = \eta^s E_{fch,t-1} + \eta^c (p_{fcht}^{g-s} + p_{fcht}^{p-s}) - \frac{1}{\eta^d} (p_{fcht}^{s-g} + p_{fcht}^{s-l}), \quad t \in \mathcal{T} \backslash \{1\} \tag{A.12}$$

$$E_{fcht} = E_0, \qquad t = 1 \tag{A.13}$$

$$\underline{E_{fh}} \le E_{fcht} \le \overline{E_{fh}}, \tag{A.14}$$

$$0 \le p_{fcht}^{s-g} + p_{fcht}^{p-g} \le \overline{p_{fh}^{pv}}, \tag{A.15}$$

$$0 \le p_{fcht}^{p-s} \le \overline{p_{fh}^{\text{batt}}}, \tag{A.16}$$

$$0 \le p_{fcht}^{g-s} \le \beta\, \overline{p_{fh}^{\text{batt}}}, \tag{A.17}$$

$$0 \le p_{fcht}^{s-g} \le \gamma\, \overline{p_{fh}^{\text{batt}}}, \tag{A.18}$$

$$0 \le p_{fcht}^{s-l} \le \overline{p_{fh}^{\text{batt}}}. \tag{A.19}$$

In this model, the objective (A.4) aims at minimizing the cost of the electricity transactions with the distribution grid, where $\lambda_t^{\text{imp}}, \lambda_t^{\text{exp}}$ are the unit electricity tariff for imported and exported energy at time t, $p_{fcht}^{\text{imp}}, p_{fcht}^{\text{exp}}$ are the imported/exported electricity from/to the single-family home at time t, respectively. The power required to meet the load excess is constrained in (A.5), where p_{fcht}^{g-l} is the power supplied to the load from the grid, p_{fcht}^{s-l} is the power supplied to the load from the battery, and p_{fcht}^{l+} is the load excess calculated as in (A.7). The PV surplus balance is given in (A.6), where p_{fcht}^{p-g} is the solar generation injected to the grid, p_{fcht}^{p-s} is the excess solar generation to charge the battery, and p_{fcht}^{l-} is the generation excess obtained as in (A.8). The balance at the distribution grid connection point is given by (A.9), where p_{fcht}^{g-s} is the charging power flow from the grid, and p_{fcht}^{s-g} is the power injection from the battery to the grid. The battery charge limits are given by (A.10), where $\overline{p_{fh}^{\text{batt}}}$ is the maximum charging flow. The battery discharge limits is constrained by (A.11), where k limits the battery discharge, and is calculated as the ratio between the battery maximum discharge duration and the time span of the tariff peak period. The energy stored in the battery is calculated by the state Eq. (A.12), where η^s, η^c, η^d are the self-discharge rate, charge efficiency, and discharge efficiency, respectively. The initial energy stored is indicated in (A.13). In this application, no condition is imposed for the energy stored at the end of the horizon, and batteries are expected to be fully discharged at that time. The battery storage limits are modeled in (A.14), where E_{fcht} is the energy stored at time t, and $\overline{E_{fh}}, \underline{E_{fh}}$ are the maximum and minimum storage limits. The maximum power flow to be injected to the grid is given by (A.15), where the combined injection from solar and battery must not exceed the solar generation nameplate capacity $\overline{p_{fh}^{pv}}$. The power flow from the solar generation to the battery is given in (A.16). The charge from the grid is controlled by (A.17), where β is a binary parameter that enables grid charging ($\beta = 0$ for no-grid charge; $\beta = 1$, otherwise). The discharge to the grid is bounded by (A.18), where γ is a binary parameter that enables discharge to the grid ($\gamma = 0$ for no-grid discharge; $\gamma = 1$, otherwise). Finally, the battery discharge to the load is limited by the battery maximum power output in (A.19).

The net load p_{fcht}^{net} is then calculated for each home h in feeder f, at time t, in scenario c, based on the optimization results as,

$$p_{fcht}^{\text{net}} = p_{fcht}^{\text{imp}} - p_{fcht}^{\text{exp}}, \quad \forall t, c, h, f. \tag{A.20}$$

Appendix B. Selection of planning days

From the previous step, net load profiles for a complete year are obtained for each feeder. The investment planning is evaluated over a set of days that capture extreme and average daily demand scenarios for each of the feeders under study. The maximum net load day, the minimum net load day, and the average net load day are considered as the planning days for the investment analysis, which are identified as explained below. The identification of these planning days aims to capture different stress conditions for the distribution grid, given that planning is driven by high coincident load and generation injection, which lead to line overloads and large voltage deviations. The feeder maximum net-load day ($D_f^{\max}$) corresponds to the day that includes the hour with the highest hourly demand of the year, normally related to a day of high consumption with low solar generation,

$$D_{fc}^{\max} = \text{day of}\left(\arg\max_t \left\{ \sum_h p_{fcht}^{\text{net}} \right\}\right). \tag{B.1}$$

The feeder minimum net-load day ($D_f^{\min}$) corresponds to the day where the lowest hourly demand is registered, generally related to a day with a low demand and a high injection from solar generation,

$$D_{fc}^{\min} = \text{day of}\left(\arg\min_t \left\{ \sum_h p_{fcht}^{\text{net}} \right\}\right). \tag{B.2}$$

To determine the average net load day (D_f^{avg}), the net load profile for each individual day is extracted and then averaged. Let $\mathbf{P}_d = [p_{t_d(1)}^{\text{net}}, \dots, p_{t_d(i)}^{\text{net}}, \dots, p_{t_d(24)}^{\text{net}}]$ be the net load profile of day d. The average net load profile, $\mathbf{P}^{\text{avg}}$ is calculated as:

$$\mathbf{P}^{\text{avg}} = \frac{1}{365} \sum_{\forall d} \mathbf{P}_d. \tag{B.3}$$

Then, the mean squared error between the averaged profile obtained and the load profile for each individual day is computed. The mean squared error is given by:

$$MSE_d = \|\mathbf{P}_d - \mathbf{P}^{\text{avg}}\|, \qquad d = \{1, \dots, 365\}. \tag{B.4}$$

Finally, the day with the minimum mean squared error is considered as the day of the average net load,

$$D_f^{\text{avg}} = \arg\min_d \left\{ MSE_d \right\}. \tag{B.5}$$

Appendix C. Least-cost optimization expansion planning model

The investment planning for each feeder under the selected scenarios is carried out using a least-cost optimization approach for distribution grid expansion. The model considers the net load profiles resulting from each of the considered battery operation strategies, and decides on line reconductoring siting and sizing, voltage regulators siting, and transformer upgrading when required. The selected planning days for each profile are considered as inputs for the model, weighted accordingly to accumulate and represent a one-year planning horizon. The optimization model for the grid expansion model is formulated in (C.1)–(C.14).

$$\min \quad IC^{rc} + IC^{tr} + IC^{vr} + \sum_{t\in\mathcal{T}} \sum_{n\in\mathcal{B}} C^{imb} \omega_t (p_{nt}^{I,+} + p_{nt}^{I,-} + q_{nt}^{I,+} + q_{nt}^{I,-}), \tag{C.1}$$

s.t.,

$$IC^{rc} = \sum_{l\in\mathcal{L}^{rc}} \sum_{r\in\mathcal{R}_l} x_{lr}^{rc}\, C_{lr}^{rc}\, cap_r^{rc}\, \frac{\delta}{1-(1+\delta)^{-L_r}}, \tag{C.2}$$

$$IC^{tr} = \sum_{l\in\mathcal{L}^{tr}} C_l^{tr,u} x_l^{tr,u} \frac{\delta}{1-(1+\delta)^{-L_{tr}}}, \tag{C.3}$$

$$IC^{vr} = \sum_{l\in\mathcal{L}^{vr}} C_l^{vr} x_l^{vr} \frac{\delta}{1-(1+\delta)^{-L_{vr}}}, \tag{C.4}$$

$$\sum_{g\in\mathcal{B}_n^s} p_{gt}^s + \sum_{l\in\mathcal{B}_n^{to}} f_{lt}^p - \sum_{l\in\mathcal{B}_n^{fr}} f_{lt}^p - p_{nt}^l - \sum_{l\in\mathcal{B}_n^{fr}} bl_{lt}^{p,fr} - \sum_{l\in\mathcal{B}_n^{to}} bl_{lt}^{p,to} + p_{nt}^{I,+} - p_{nt}^{I,-} = 0, \quad \forall n\in\mathcal{B}, t\in\mathcal{T}, \tag{C.5}$$

$$\sum_{g\in\mathcal{B}_n^s} q_{gt}^s + \sum_{l\in\mathcal{B}_n^{to}} f_{lt}^q - \sum_{l\in\mathcal{B}_n^{fr}} f_{lt}^q - q_{nt}^l - \sum_{l\in\mathcal{B}_n^{fr}} bl_{lt}^{q,fr} - \sum_{l\in\mathcal{B}_n^{to}} bl_{lt}^{q,to} + q_{nt}^{I,+} - q_{nt}^{I,-} = 0, \quad \forall n\in\mathcal{B}, t\in\mathcal{T}, \tag{C.6}$$

$$-cap_l^{s,max} cap^{th} \le f_{lt}^p \le cap_l^{s,max} cap^{th}, \quad \forall l\in\mathcal{L}^{rc}, t\in\mathcal{T}, \tag{C.7}$$

$$-cap_l^{s,max} cap^{th} \le f_{lt}^q \le cap_l^{s,max} cap^{th}, \quad \forall l\in\mathcal{L}^{rc}, t\in\mathcal{T}, \tag{C.8}$$

$$v_{to(l),t}^{\dagger} - \left[v_{fr(l),t}^{\dagger} - 2(R_l f_{lt}^p + X_l f_{lt}^q)\right] = 0, \quad \forall l\in\mathcal{L}, t\in\mathcal{T}, \tag{C.9}$$

$$v_n^{min^2} \le v_{nt}^{\dagger} \le v_n^{max^2}, \quad \forall n\in\mathcal{B}, t\in\mathcal{T}, \tag{C.10}$$

$$-cap_l^{tr} \le f_{lt}^p \le cap_l^{tr}, \quad \forall l\in\mathcal{L}^{tr}, t\in\mathcal{T}, \tag{C.11}$$

$$-cap_l^{tr} \le f_{lt}^q \le cap_l^{tr}, \quad \forall l\in\mathcal{L}^{tr}, t\in\mathcal{T}, \tag{C.12}$$

$$cap_l^{tr} \le cap_l^{tr,max} + M\ x_l^{tr,u}, \quad \forall l\in\mathcal{L}^{tr}, \tag{C.13}$$

$$v_{to(l),t}^{\dagger} - \left[v_{fr(l),t}^{\dagger,mid} - 2(R_l f_{lt}^p + X_l f_{lt}^q)\right] = 0, \quad \forall l\in\mathcal{L}^{tr,vr}, t\in\mathcal{T}. \tag{C.14}$$

The optimization model minimizes the annualized investment costs of line reconductoring (IC^{rc}), transformer upgrading (IC^{tr}), voltage regulator installation (IC^{vr}). The function also includes a very high cost (C^{imb}) to enforce power balance as soft constraints, where the power flow imbalances $p_{nt}^{I,+}$, $p_{nt}^{I,-}$, $q_{nt}^{I,+}$, $q_{nt}^{I,-}$ are positive auxiliary variables. The annualized cost of line reconductoring is calculated in (C.2), where x_{lr}^{rc} is the binary variable that decides if reconductoring of section l with option r is implemented, C_{lr}^{rc} is the cost of reconductoring section l with option r, cap_r^{rc} is the line capacity of option r, L_r is the service life of option r conductor, δ is the discount rate, $\mathcal{L}^{rc}$ is the subset of candidate line sections for reconductoring, and $\mathcal{R}_l$ is the set of reconductoring options for section l. The annualized investment cost of transformer upgrading is obtained in (C.3), where $x_l^{tr,u}$ is the binary decision variable that indicates if a transformer located in section l is upgraded, $C_l^{tr,u}$ is the cost of upgrading transformer in section l, L_{tr} is the transformer service life, and $\mathcal{L}^{tr}$ is the subset of sections that contain a transformer. Finally, the annualized investment cost on voltage regulators is determined in (C.4), where x_l^{vr} is a binary variable that indicates if a voltage regulator is to be installed in section l, C_l^{vr} is the cost of installing a voltage regulator in section l, L_{vr} is the voltage regulator service life, and $\mathcal{L}^{vr}$ is the subset of candidate sections to install voltage regulators. Unit costs for distribution system upgrades were taken from the NREL's Distribution Grid Integration Unit Cost Database (Horowitz, 2019), which contain a set of real distribution component costs provided by US utilities.

The energy balance is formulated based on the linear approximation of the DistFlow model (Baran and Wu, 1989). The active and reactive power flow balance as shown in (C.5)–(C.6), respectively, where p_{gt}^s, q_{gt}^s are the active/reactive power injected by the substation at node g, time t, f_{lt}^p, f_{lt}^q are the active/reactive power flow in line l, time t, p_{nt}^l, q_{nt}^l are the active/reactive loads at node n, time t, $bl_{lt}^{p,fr}, bl_{lt}^{p,to}$ are auxiliary variables related to line losses. $\mathcal{B}_n^s$ is the subset of substations connected to node n, $\mathcal{B}_n^{to}$ is the subset of nodes with node n indicated as their end node, and $\mathcal{B}_n^{fr}$ is the subset of nodes with node n indicated as their start node. Line power flow limits are represented as a function of the line capacity as specified by (C.7)–(C.8), where $cap_l^{s,max}$ is the maximum capacity of line l, and cap^{th} is the overload limit. The voltage drop in each line is defined by (C.9), where $v_{to(l),t}^{\dagger}$ is the voltage at end node of line t, $v_{fr(l),t}^{\dagger}$ is the voltage at start node in line t, and R_l, X_l are the resistance and reactance of line l, respectively. The voltage limits are defined in (C.10), where $v_{nt}^{\dagger}$ is the squared voltage at node n, time t, and v_n^{min}, v_n^{max} are the minimum and maximum voltage magnitude limits, respectively.

Constraints related to transformer upgrading and voltage regulator installation are given in (C.11)–(C.14). The active and reactive power flow limits are defined in (C.11)–(C.12), where cap_l^{tr} is a positive variable representing the transformer capacity defined in (C.13), $cap_l^{tr,max}$ is the transformer current maximum capacity, and M is a large value, and $\mathcal{L}^{tr}$ is the subset of sections with transformers. The voltage drop in sections with voltage regulators and transformers is modeled in (C.14), where $v_{fr(l),t}^{\dagger,mid}$ is the squared voltage after tap for transformers and voltage regulators, and $\mathcal{L}^{tr,vr}$ is the subset of line sections where voltage regulators or transformers are added.

Data availability

The data used in this study are publicly available from the sources cited in the manuscript.

References

Ackermann, T., Knyazkin, V., 2002. Interaction between distributed generation and the distribution network: operation aspects. In: IEEE/PES Transmission and Distribution Conference and Exhibition. vol. 2, pp. 1357–1362 vol.2. http://dx.doi.org/10.1109/TDC.2002.1177677.

Alam, M.J.E., Muttaqi, K.M., Sutanto, D., 2013. Mitigation of rooftop solar PV impacts and evening peak support by managing available capacity of distributed energy storage systems. IEEE Trans. Power Syst. 28 (4), 3874–3884. http://dx.doi.org/10.1109/TPWRS.2013.2259269.

Babacan, O., Torre, W., Kleissl, J., 2017. Siting and sizing of distributed energy storage to mitigate voltage impact by solar PV in distribution systems. Sol. Energy 146, 199–208. http://dx.doi.org/10.1016/j.solener.2017.02.047.

Baran, M., Wu, F., 1989. Optimal sizing of capacitors placed on a radial distribution system. IEEE Trans. Power Deliv. 4 (1), 735–743. http://dx.doi.org/10.1109/61.19266.

Barbose, G.L., Darghouth, N.R., O'Shaughnessy, E., Forrester, S., 2024. Tracking the Sun: Pricing and Design Trends for Distributed Photovoltaic Systems in the United States, 2024 Edition. Technical Report, Lawrence Berkeley National Laboratory, (Accessed 6 June 2025).

Blonsky, M., Maguire, J., McKenna, K., Cutler, D., Balamurugan, S.P., Jin, X., 2021. OCHRE: The object-oriented, controllable, high-resolution residential energy model for dynamic integration studies. Appl. Energy 290, 116732. http://dx.doi.org/10.1016/j.apenergy.2021.116732.

California Public Utilities Commission, 2023. Electrification Impacts Study Part 1: Bottom-Up Load Forecasting and System-Level Electrification Impacts Cost Estimates. Technical Report.

Dennis, P., Passey, R., Samhan, M.S., Yildiz, B., 2025. Neighbourhood-scale battery energy storage system revenue optimisation in distribution networks: Impact of price forecasts. Energy Rep. 14, 3204–3220. http://dx.doi.org/10.1016/j.egyr.2025.10.011.

Edison Electric Institute, 2024. EEI industry capital expenditures with functional detail.

Forrester, S., Satchwell, A., Barbose, G.L., Cappers, E., Miller, C., Alberg, A., 2024. Retail electricity price and cost trends: 2024 update. (Accessed 6 June 2025).

Gagnon, P., Pham, A., Cole, W., Awara, S., Barlas, A., Brown, M., Brown, P., Carag, V., Cohen, S., Hamilton, A., Ho, J., Inskeep, S., Karmakar, A., Lavin, L., Lopez, A., Mai, T., Mowers, J., Mowers, M., Murphy, C., Pinchuk, P., Schleifer, A., Sergi, B., Steinberg, D., Williams, T., 2023. 2023 Standard Scenarios Report: A U.S. Electricity Sector Outlook. Technical Report, (NREL/TP-6A40-87724), National Renewable Energy Laboratory (NREL), Golden, CO.

Gupta, R., Pena-Bello, A., Streicher, K.N., Roduner, C., Farhat, Y., Thöni, D., Patel, M.K., Parra, D., 2021. Spatial analysis of distribution grid capacity and costs to enable massive deployment of PV, electric mobility and electric heating. Appl. Energy 287, 116504. http://dx.doi.org/10.1016/j.apenergy.2021.116504.

Hill, C.A., Such, M.C., Chen, D., Gonzalez, J., Grady, W.M., 2012. Battery energy storage for enabling integration of distributed solar power generation. IEEE Trans. Smart Grid 3 (2), 850–857. http://dx.doi.org/10.1109/TSG.2012.2190113.

Horowitz, K., 2019. Distribution system upgrade unit cost database current version. United States. URL doi:10.7799/1491263.

Horowitz, K.A.W., Ding, F., Mather, B.A., Palmintier, B.S., 2018. The Cost of Distribution System Upgrades to Accommodate Increasing Penetrations of Distributed Photovoltaic Systems on Real Feeders in the United States. Technical Report, NREL, http://dx.doi.org/10.2172/1432760.

Horowitz, K.A., Palmintier, B., Mather, B., Denholm, P., 2018. Distribution system costs associated with the deployment of photovoltaic systems. Renew. Sustain. Energy Rev. 90, 420–433. http://dx.doi.org/10.1016/j.rser.2018.03.080.

Koivisto, M., Das, K., Guo, F., Sørensen, P., Nuño, E., Cutululis, N., Maule, P., 2019. Using time series simulation tools for assessing the effects of variable renewable energy generation on power and energy systems. WIREs Energy Environ. 8 (3), e329. http://dx.doi.org/10.1002/wene.329.

Lee, J., Bérard, J.-P., Razeghi, G., Samuelsen, S., 2020. Maximizing PV hosting capacity of distribution feeder microgrid. Appl. Energy 261, 114400. http://dx.doi.org/10.1016/j.apenergy.2019.114400.

McAllister, R., Manning, D., Bird, L., Coddington, M., Volpi, C., 2019. New Approaches to Distributed PV Interconnection: Implementation Considerations for Addressing Emerging Issues. Technical Report, (NREL/TP-6A20-72038), National Renewable Energy Laboratory (NREL), Golden, CO, URL https://www.nrel.gov/docs/fy19osti/72038.pdf.

Morell Dameto, N., Chaves-Ávila, J.P., Gómez San Román, T., 2020. Revisiting electricity network tariffs in a context of decarbonization, digitalization, and decentralization. Energies 13 (12), http://dx.doi.org/10.3390/en13123111.

Morell-Dameto, N., Chaves-Ávila, J.P., Gomez San Roman, T., Duenas-Martinez, P., Schittekatte, T., 2024. Network tariff design with flexible customers: Ex-post pricing and a local network capacity market for customer response coordination. Energy Policy 184, 113907. http://dx.doi.org/10.1016/j.enpol.2023.113907.

Okafor, C.E., Gbadamosi, S.L., Krishnamurthy, S., Ratshitanga, M., Moodley, P., 2025. Techno-economic analysis of battery storage technologies in distribution networks with integrated electric vehicles and solar PV systems. Energy Rep. 14, 579–599. http://dx.doi.org/10.1016/j.egyr.2025.06.008.

Open Energy Data Initiative, 2020. SMART-DS: Synthetic multi-agent residential test distribution system. Available via the Open Energy Data Initiative's AWS S3 Explorer.

Palmintier, B., Broderick, R., Mather, B., Coddington, M., Baker, K., Ding, F., Reno, M., Lave, M., Bharatkumar, A., 2016. On the Path to SunShot: Emerging Issues and Challenges in Integrating Solar with the Distribution System. Technical Report, (NREL/TP-5D00-65331), National Renewable Energy Laboratory (NREL).

Palmintier, B., Mateo Domingo, C., Postigo Marcos, F.E., Gomez San Roman, T., de Cuadra, F., Gensollen, N., Elgindy, T., Duenas, P., 2020. SMART-DS synthetic electrical network data OpenDSS models for SFO, GSO, and AUS.

Solar Energy Industries Association, 2025. Solar industry research data. URL https://seia.org/research-resources/solar-industry-research-data/, (Accessed 6 June 2025).

Su, L., Gang, W., Liu, M., Ling, Z., Zhang, Y., Dong, S., 2025. A capacity optimization method for the battery energy storage system based on historical electricity data of existing buildings. Energy Rep. 13, 6132–6147. http://dx.doi.org/10.1016/j.egyr.2025.05.060.

U.S. Energy Information Administration, 2024. Grid infrastructure investments drive increase in utility spending over last two decades. URL https://www.eia.gov/todayinenergy/detail.php?id=63724.

Wood, E., Borlaug, B., Moniot, M., Lee, D.-Y., Ge, Y., Yang, F., Liu, Z., 2023. The 2030 National Charging Network: Estimating U.S. Light-Duty Demand for Electric Vehicle Charging Infrastructure. Technical Report, National Renewable Energy Laboratory (NREL), http://dx.doi.org/10.2172/1988020, URL https://www.osti.gov/biblio/1988020.